Invariant Relationships in Side-Looking Synthetic Aperture Radar Imagery

Nils N. Haag
Science Applications International Corporation, 700 South Babcock Street, Melbourne, FL 32901
Michael H. Brill
Science Applications International Corporation, 1710 Goodridge Drive 1-11-1, P.O. Box 1303, McLean, VA 22102
Eamon B. Barrett
Lockheed Missiles and Space Company, 1111 Lockheed Way, 061–40, B–107, Sunnyvale, CA 94089–3504

ABSTRACT: The purpose of this article is to describe a relationship that enables one to match a set of image-point coordinates in a pair of strip-mapping synthetic-aperature radar (SAR) images with a corresponding set of object-point coordinates without resorting to resection or triangulation, i.e., to classify the image points and the object points as being a match or a mismatch. This relationship is invariant and is shown, for an actual imaging system, to be independent of the exterior orientation of the SAR and of the rotation and translation of the object. Two SAR images covering five object points suffice to define this invariant quantity. The quantity so defined is a volume ratio (in object space) of the tetrahedra spanned by two subsets of four of the five points. The result of this study, which is based on simulated imagery, demonstrates that for the actual imaging system under consideration one can in theory use the invariance relationship to detect misidentified ground control points in a single image. Other potential applications of the invariance relationship, such as the classification of an object in a single SAR image, are also addressed.

INTRODUCTION

THE PURPOSE OF THIS STUDY is to develop an invariance relationship for strip-mapping synthetic-aperture radar (SAR) imagery, and to apply it to the problem of comparing image coordinates and object coordinates (classification). The key to this invariance relationship is the fact that ratios of volumes defined by sets of points in three-dimensional object space are invariant under "perspective" transformation into two-dimensional SAR images. A general formulation of the invariance relationship will be developed, and also a special formulation for the STAR-1 synthetic-aperature radar system (Nichols *et al.*, 1986). Furthermore, a simulation example will be presented that uses the invariance relationship to detect misidentified ground control in a single STAR-1 image. The geometrical aspects particular to the SAR collection will be discussed, and other potential applications will be suggested.

A SAR image is similar to a familiar optical image in that it encodes information from a three-dimensional object space in two dimensions. Because three dimensions are encoded in two, the encoding is ambiguous, and more than one image of the same object is needed to resolve the ambiguities. The nature of the ambiguities, however, is quite different for SAR and for optical images.

In an optical image, the two image coordinates (x,y) determine a line of sight from the camera station to the object point (Duda and Hart, 1973). From a single image of the object point, it is possible to ascertain only the point's line of sight, and not its position along the line of sight. Triangulation (intersection of lines of sight to the point from several images with known acquisition parameters) is necessary to determine the object point's three-dimensional coordinates.

In a SAR image, the object-space point is determined to be on a particular *circle* (called a projection circle) instead of on a line of sight. This projection circle is the intersection of a sphere centered on the acquiring platform (called the range sphere, whose radius is known because radar measures the round-trip travel time of a pulse) and a plane perpendicular to the velocity vector of the platform. This plane arises from the intersection of the range sphere with the cone of constant frequency dilation (which is determined by a SAR Doppler measurement that is independent of the range measurement). In spotlight-mode SAR (Ausherman *et al.*, 1984; Brill, 1987) the phase-history data for an entire image is acquired and then the Dopplers and ranges are sorted to make an image. In strip-mapping SAR (Munson and Visentin, 1989), the image is acquired one projection-circle plane at a time, with evolving time t as one of the image coordinates and slant range R as the other. Both kinds of SAR have the same geometry insofar as the ambiguity in the image is concerned: the curve of ambiguity is a projection circle. It is possible to retrieve the three-dimensional coordinates of an object point by intersecting the projection circles from several images whose acquisition geometries are known. The determination of the acquisition geometries, called resection, requires some ground-truth information in the form of control points.

In the absence of resection, it is still possible to obtain usable information about the objects imaged in optical and SAR images. For optical images procedures exist called *relative orientation* to extract such information from several images (Slama, 1980). In the present paper we introduce a kind of relative orientation that can be used for strip-mapping SAR imagery. The method involves finding relationships between the image coordinates (on several images) of several object points, such that the evaluation of these relationships does not depend on the acquisition parameters of the images. In object space, the relationships are simply ratios of the volumes of tetrahedra defined by the object-space points. These volume ratios are computable from image measurements because they are equal to ratios of determinants involving measured values of R and t from two images of these same object points. Because of the acquisition-invariance, the method can be used to classify objects by comparing the relationships computed from radar image-point measurements with relationships computed between points for a menu of known objects. There is one important constraint on the method: The two platform velocities must be nonparallel to each other.

This article will develop the basic theory, present an illustrative example using computer simulation, and identify the aspects of strip-mapping SAR that render it particularly amenable to our analysis (as compared with frame optical imagery—see Barrett *et al.* (1991)). Testing of the concept on actual SAR images is deferred to future study.

PHOTOGRAMMETRIC ENGINEERING & REMOTE SENSING,
Vol. 57, No. 7, July 1991, pp. 927–931.

0099-1112/91/5707–927$03.00/0

GENERAL FORMULATION

To reach the objective of computing object-point relationships from image measurements, our mathematical method will be (a) to write the condition equations of strip-mapping SAR; (b) to extract from the full set of condition equations all the equations that are linear functions of the object-space coordinates; (c) to rearrange these linear condition equations until the coefficients of the object-space coordinates all depend on image-acquisition parameters but *not* on which object-space point is considered; (d) to note that the inhomogeneous term of each of the linear condition equations is the sum of a term that depends only on image-acquisition parameters and a term that depends on measured image coordinates (R,t) but not on the unknown image-acquisition parameters; and (e) to note therefore that a ratio of determinants of measurement vectors among the image-space points is the same as a ratio of volumes of tetrahedra subtended by the points in object space. Along the way, the geometric significance of the various equations will be noted.

First of all, we write the condition equations of strip-mapping SAR. Let the image index be i, where $i=1,2$; also, let $\mathbf{X}_j$ be the position of object-space point j. The image coordinates of $\mathbf{X}_j$ in image i are given by a slant range R_{ij} and a time t_{ij} (measured from a zero of time that is near the center of the ith imaging window). The ith platform moves with velocity $\mathbf{v}_i$ (whose magnitude v_i is assumed known and which is assumed constant over the time of acquisition of the image), and starts out at position $\mathbf{S}_i$ when the ith imaging time is zero. The Doppler-cone angle of the ith platform is θ_i. Given these definitions, the condition equation for the slant range is

$$R_{ij}^2 = (\mathbf{X}_j - \mathbf{S}_i - \mathbf{v}_i\, t_{ij})^2 \tag{1}$$

and the constant-Doppler condition equation is

$$R_{ij}\, u_i = (\mathbf{X}_j - \mathbf{S}_i - \mathbf{v}_i\, t_{ij}) \cdot \mathbf{v}_i, \tag{2}$$

where $u_i = v_i \cos\theta_i$. The geometry underlying these equations is illustrated in Figure 1 (for the special case of broadside viewing, in which $\theta_i = 90°$). Equation 1 defines the range sphere for point j on image i, and Equation 2 defines the plane perpendicular to the ith velocity vector that passes through the point $\mathbf{X}_j$ and also through the instantaneous platform position $\mathbf{S}_i + \mathbf{v}_i\, t_{ij}$. given R_{ij}, t_{ij}, $\mathbf{S}_i$, and $\mathbf{v}_i$, the point $\mathbf{X}_j$ is constrained to lie on a circle that is the intersection of the sphere defined by Equation 1 and the plane defined by Equation 2. This circle is the *projection circle* of point j as constrained by image i. Correspondingly, the plane defined by Equation 2 is the ith *projection-circle plane* through point j. Of course, because neither the direction of $\mathbf{v}_i$ nor the position $\mathbf{S}_i$ are known in the present problem, the identity of the projection circle for image i is also unknown.

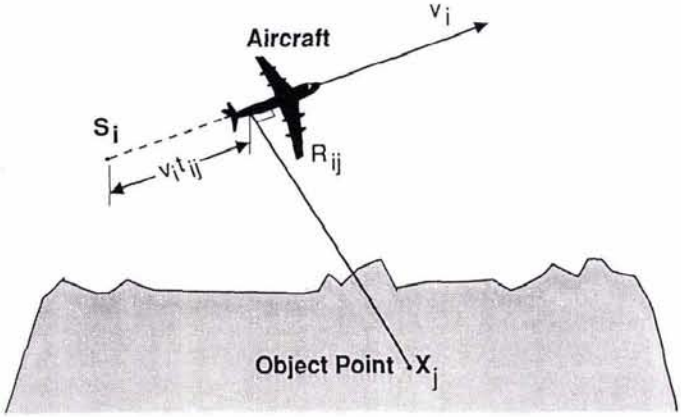

FIG. 1. Strip-mapping SAR acquisition geometry.

The second step in our method is to extract from Equations 1 and 2 (which comprise *four* equations, two for $i=1$ and two for $i=2$) as many equations as possible that are linear in the coordinates (X_j, Y_j, Z_j) of point $\mathbf{X}_j$. No further work needs to be done to Equation 2, for it is already linear in $\mathbf{X}_j$. Equation 1 is nonlinear in $\mathbf{X}_j$, but it actually represents two range conditions (for $i = 1,2$), and hence a single linear equation in $\mathbf{X}_j$ can be retrieved by subtracting Equation 1 for $i=1$ from Equation 1 for $i=2$:

$$(R_{2j}^2 - R_{1j}^2) - (\mathbf{S}_2 + \mathbf{v}_2\, t_{2j})^2 + (\mathbf{S}_1 + \mathbf{v}_1\, t_{1j})^2 = 2\,(\mathbf{S}_1 - \mathbf{S}_2 + \mathbf{v}_1\, t_{1j} - \mathbf{v}_2\, t_{2j}) \cdot \mathbf{X}_j. \tag{3}$$

This equation also defines a plane, and it is the plane containing the circle of intersection of the range spheres.

Taken together, Equation 2 for $i=1,2$ (representing the two projection-circle planes) and Equation 3 (representing the plane of range-sphere intersection) constitute three linear equations in the object-space coordinates (X_j, Y_j, Z_j).

The third step in our method is to rearrange Equations 2 and 3 so that the coefficients of $\mathbf{X}_j$ depend only on the acquisition parameters (i-dependence), and not on the object-space point (j-dependence). Equation 2 satisfies this condition, for $i=1, 2$. Equation 3 can be made to satisfy the condition, by subtracting from it $2t_{1j}$ multiplied by Equation 2 for $i=1$, and then adding to it $2t_{2j}$ multiplied by Equation 2 for $i=2$. The result is as follows:

$$R_{2j}^2 - R_{1j}^2 + v_2^2\, t_{2j}^2 + 2\, R_{2j}\, u_2\, t_{2j} - v_1^2 t_{1j}^2 - 2\, R_{1j}\, u_1\, t_{1j} \equiv p_{12j} = S_2^2 - S_1^2 - 2(\mathbf{S}_2 - \mathbf{S}_1) \cdot \mathbf{X}_j, \tag{4}$$

where S_1 and S_2 are the magnitudes of the position vectors $\mathbf{S}_1$ and $\mathbf{S}_2$. For compactness of notation, we have defined p_{12j} as the left-hand side of Equation 4.

The fourth step in our method is to examine the inhomogeneous terms in Equations 2 and 4. It can be seen that the inhomogeneous term in Equation 2 does not depend on acquisition parameters other than the known value v_i. The inhomogeneous term in Equation 4, on the other hand, consists of the term p_{12j} that depends only on the measured image coordinates (and of course on v_i^2 and on θ_i), and also a term on the right-hand side that depends only on the acquisition parameters and not on the object-space point j.

The fifth step in our method is to rewrite Equations 2 and 4 in a vector form so a 4-vector of measured and known quantities occur on the left-hand side and a 4 by 4 matrix multiplied by the enhanced vector $(1,\mathbf{X}_j)$ occurs on the right-hand side. Determinants of the left- and right-hand sides will then reveal the desired theorem. A convenient first step is to rewrite Equation 2 as follows:

$$v_i^2\, t_{ij} + R_{ij}\, u_i \equiv q_{ij} = -\mathbf{S}_i \cdot \mathbf{v}_i + \mathbf{v}_i \cdot \mathbf{X}_j. \tag{5}$$

Once again, for compactness of notation, we have defined q_{ij} as the left-hand side of Equation 5.

Now Equation 4 can be written as one vector component of a linear system, and Equation 5 for $i = 1$ and 2 can be written as two other vector components. A fourth equation (the first in the system below) is an identity. The vector equation is

$$\mathbf{G}_j = \mathbf{F} \begin{bmatrix} 1 \\ X_j \\ Y_j \\ Z_j \end{bmatrix} \tag{6}$$

where $\mathbf{F}$ is the 4 by 4 matrix

$$\mathbf{F}=\begin{bmatrix} 1 & 0 & 0 & 0 \\ (S_2^2-S_1^2) & -2(S_{2x}-S_{1x}) & -2(S_{2y}-S_{1y}) & -2(S_{2z}-S_{1z}) \\ -\mathbf{S}_1\cdot\mathbf{v}_1 & v_{1x} & v_{1y} & v_{1z} \\ -\mathbf{S}_2\cdot\mathbf{v}_2 & v_{2x} & v_{2y} & v_{2z} \end{bmatrix} \tag{7}$$

and $\mathbf{G}_j$ is the column 4-vector

$$\mathbf{G}_j = (1, p_{12j}, q_{1j}, q_{2j})^T. \tag{8}$$

Here, once again, $\mathbf{G}_j$ is a function of only the measurements R_{ij}, t_{ij} and of the known values v_i and θ_i in each image i, and $\mathbf{F}$ is constant for the two images.

Now consider four object points $j=1,2,3,4$. Then, from Equation 6,

$$(\mathbf{G}_1, \mathbf{G}_2, \mathbf{G}_3, \mathbf{G}_4) = \mathbf{F}\begin{bmatrix} 1 & 1 & 1 & 1 \\ X_1 & X_2 & X_3 & X_4 \\ Y_1 & Y_2 & Y_3 & Y_4 \\ Z_1 & Z_2 & Z_3 & Z_4 \end{bmatrix}. \tag{9}$$

Because the matrix on the right-hand side of Equation 9 is equal to the matrix on the left, their determinants are equal. The determinantal equation is

$$D_{1234} = \det(\mathbf{F})\, V_{1234}, \tag{10}$$

where

$$D_{1234} = \det(\mathbf{G}_1, \mathbf{G}_2, \mathbf{G}_3, \mathbf{G}_4) \tag{11}$$

is the determinant of the left-hand side of Equation 9, and

$$V_{1234} = \det\begin{bmatrix} 1 & 1 & 1 & 1 \\ X_1 & X_2 & X_3 & X_4 \\ Y_1 & Y_2 & Y_3 & Y_4 \\ Z_1 & Z_2 & Z_3 & Z_4 \end{bmatrix} \tag{12}$$

is six times the volume of the tetrahedron formed by the four object points 1,2,3,4. In other words, the determinant of the matrix containing only measurements of four points in two images is proportional (by the factor 6 det[**F**]) to the volume of a tetrahedron formed by the points. By considering a set of five points, one can cancel the constant of proportionality, and write

$$\frac{D_{1234}}{D_{1235}} = \frac{V_{1234}}{V_{1235}}, \tag{13}$$

and so forth. This is the desired theorem relating measurements on the left-hand side of the equation to volumes formed from sets of object points on the right-hand side of the equation. The left-hand side of the equation will be referred to as the *D*-ratio and the right-hand-side as the *V*-ratio.

SPECIAL FORMULATION

The general formulation above requires prior knowledge of the Doppler cone angle θ_i and the speed of the aircraft v_i. By considering the operational STAR-1 SAR system (Nichols *et al.*, 1986), one can eliminate these variables and write the measurement Equations 4 and 5 simply in terms of image pixel coordinates.

STAR-1 contains an inertial guidance system that provides velocity measurements. These measurements are filtered, and the difference between the filtered velocity and measured velocity is used by the real-time signal processor to construct lines of imagery that are parallel and perpendicular to the filtered velocity vector. Because of the characteristics of the filter, the direction of the filtered vector changes slowly and may be assumed constant over short periods of time. This being the case, one may then assume that $\mathbf{v}_i$ represents the filtered velocity vector and $\theta_i = 90°$. One can then set $u_i = 0$ in the measurement equations.

STAR-1 clocks out the lines of imagery at a rate depending on the forward speed of the aircraft. This achieves a constant pixel width in the direction of flight. Because we have assumed that the aircraft position changes linearly with time, we can write

$$v_i t_{ij} = l_{ij}\, \Delta l, \tag{14}$$

where l_{ij} is the image line number for point j in image i, and Δl is the ground pixel width in the in-flight direction.

The range from the aircraft to a ground point in the STAR-1 system can be written as

$$R_{ij} = R_o + s_{ij}\, \Delta s, \tag{15}$$

where R_o is a constant range delay (range from the aircraft to the first ground pixel), s_{ij} is the image sample number in the slant-range plane, and Δs is the pixel width in range.

Substituting Equations 14 and 15 into Equation 4 with $u_i = 0$ and dividing through by $2R_o\Delta s$ results in a new definition of p_{12j} and also a new second row of matrix **F** in Equation 7. Because dependence on matrix **F** cancels out in our final result, we need to consider only the new expression for p_{12j}, which is

$$p_{12j} = (s_{2j} - s_{1j}) + (s_{2j}^2 - s_{1j}^2)\left(\frac{\Delta s}{2R_o}\right) + (l_{2j}^2 - l_{1j}^2)\left(\frac{\Delta l}{2R_o}\right)\left(\frac{\Delta l}{\Delta s}\right), \tag{16}$$

which depends only on the image pixel coordinates (l_{ij}, s_{ij}) and on known constants.

In a similar manner, substituting Equation 14 into Equation 5 for t_{ij} and dividing through by $v_i\Delta l$ results in a new definition of q_{ij} and a new last two rows of matrix **F**. Again, because **F**-dependence cancels out of our final result, we need consider only the new expression for q_{ij}, which is

$$q_{ij} = l_{ij}. \tag{17}$$

Equations 16, 17, 8, 11, 12, and 13 in that order constitute the theorem for the special case.

A simulation example applying these equations is presented in the following section.

A SIMULATION DETERMINING MIS-IDENTIFIED GROUND CONTROL POINTS

The simulation examples presented here are intended to show how to use the invariant relationship together with template image matching. The examples will not address subtleties of the method (but some of these subtleties are discussed in the section that follows).

The sample problem to be addressed is as follows. Given the measured image pixel coordinates of five control points identified in a STAR-1 image, and the corresponding object-space coordinates of these points, determine if one or more of the control points has been mis-identified on the image. In other words, the problem is to determine whether the object points and image points are a match or a mismatch.

To solve the problem, we introduce the idea of a template image, which may be thought of as a blueprint or drawing of how the ground points should appear from some perspective. A template image is generated from the ground-control-point object-space coordinates by applying the appropriate image projective relationships for a given (invented) acquisition geometry.

To recognize mismatches between ground control and the points in the real image, the real image is compared to the template image by combining the real image coordinates with the template image coordinates according to the left-hand side of Equation 13. If the points are correctly matched, the application of Equation 13 should yield the same value as computed from the volume ratio formed from the object-space coordinates on the right-hand side of the equation. If the volume ratio is different from the quantity derived from the image coordinates, then there is a mismatch.

Because the ratio-of-determinants theorem given by Equation 13 is independent of the exterior orientation, one is free in principle to select arbitrarily the perspective of the template image (with some constraints as are discussed in the following section).

Consider five ground-control points distributed over a 10-km by 10-km area as shown in Figure 2. The points are numbered, and their elevations (in metres) are given in parentheses. The values of the control-point coordinates are given in Table 1.

Next, consider a STAR-1 SAR, flying due southward and to the west of the area at an altitude of 33,000 feet. This SAR sensor uses the following nominal parameter values:

- range delay R_o = 20 km;
- ground pixel width in in-flight direction Δl = 4.2 metres; and
- pixel width in range Δs = 5.7 metres.

The resulting STAR-1 image coordinates (for an image labeled image 2) are given in Table 2.

For image 1, we generate a template image with a perspective we are free to choose. The perspective is chosen to be from north of the area and crossing from east to west. The resulting template image coordinates are given in Table 3.

In the first case considered (Case 1), the image coordinates and the template coordinates are combined in the left-hand side of Equation 13, forming a ratio (D-ratio) of 0.55. The same value (V-ratio) is found by evaluating the right-hand side of Equation 13 using the ground-control-point object-space coordinates. This equality of D-value and V-value ratios indicates that the image coordinates match the ground-control points.

Next, consider a case (Case 2) in which one has mis-labeled image points 4 and 5 (reversed them). This produces a D-ratio of -1.12.

Finally, consider a case (Case 3) in which image point 5 has been mis-identified by +25 pixels in sample number. This results in a D-ratio of 0.83.

The three cases are summarized in Table 4.

To produce Table 4, the standard deviation of the difference is obtained by assuming random, independent mensuration errors of one pixel (at one sigma) in line number and also in sample number, and propagating the errors to the D-ratio (using the standard technique—see, e.g., Deming (1948)). Case 1 is clearly consistent with the expected difference of zero, and therefore properly indicates a match of image measurements with the ground control. Cases 2 and 3 are clearly inconsistent with the expected difference of zero, and therefore properly indicate problems in the image measurements.

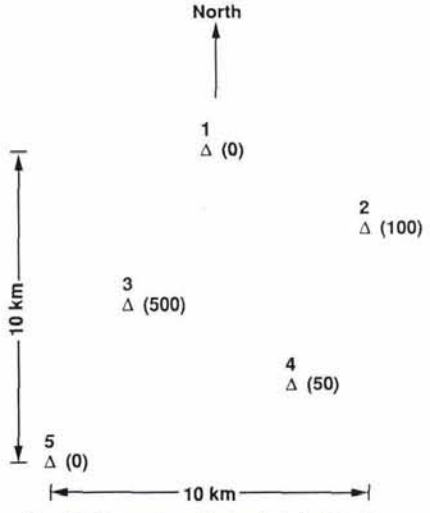

FIG. 2. Ground control-point distribution.

TABLE 1. GROUND CONTROL POINT COORDINATES.

Point (j)	X (metres)	Y (metres)	Z (metres)
1	5000	10000	0
2	10000	7500	100
3	2500	5000	500
4	7500	2500	50
5	0	0	0

GEOMETRICAL DISCUSSION

The SAR result derived above has no simple analog in frame optical imagery. In frame optical imagery, the image invariants are the more complicated cross-ratios of object-space volumes, and extraction of the invariants requires an algorithm (Barrett *et al.*, 1991) using 34 images and eight object-space points. Therefore, it is instructive to examine the geometrical aspects of SAR which render it privileged among image-gathering systems insofar as the computation of invariants is concerned.

As noted earlier (Brill and Williamson, 1989), an analog of triangulation between two SAR images can be done by solving three linear condition equations for $\mathbf{X}_j = (X_j, Y_j, Z_j)$. Solving these equations amounts to finding the intersection of three planes: the plane of the projection circle in image 1 passing through $\mathbf{X}_j$; the plane of the projection circle in image 2 passing through $\mathbf{X}_j$; and the plane of the intersection of the range spheres from image 1 and image 2, corresponding to $\mathbf{X}_j$.

TABLE 2. STAR-1 IMAGE COORDINATES OF CONTROL POINTS.

Point (j)	Line number (l_{2j})	Sample number (s_{2j})
1	0	795
2	595	1616
3	1190	353
4	1786	1202
5	2381	0

TABLE 3. TEMPLATE IMAGE COORDINATES OF CONTROL POINTS.

Point (j)	Line number (l_{1j})	Sample number (s_{1j})
1	1190	68
2	0	261
3	1786	451
4	595	794
5	2381	1105

TABLE 4. RESULTS OF STATISTICAL ANALYSIS.

Case	D-ratio minus V-ratio	Standard Deviation
1	0.00	0.03
2	−1.67	0.01
3	0.28	0.05

The first and second of these planes—the projection-circle planes—are represented by Equation 5 above, for fixed object point $\mathbf{X}_j$ and for image i = 1 or 2. The third of these planes—generated by the intersection of the range spheres—is defined by Equation 4, for object point $\mathbf{X}_j$ fixed. Note that the normal to the plane in Equation 4 is proportional to the "stereo" base $\mathbf{S}_2 - \mathbf{S}_1$.

One feature of SAR imagery that enables the evaluation of the ratio of object-space volumes is that all the planes of intersection of range spheres from the same images 1 and 2 are parallel, because they have the same normal $\mathbf{S}_2 - \mathbf{S}_1$ independent of the object point $\mathbf{X}_j$. Similarly, all the projection-circle planes from an image share a normal (the velocity vector of the vehicle generating that image), and are hence also parallel to each other, independent of the imaged object *j*. This commonality of the normal (i.e., *j*-independence of the normal) is what allows the determinant of acquisition geometry generated by matrix **F** to cancel in the ratio-of-determinants operation. The same process did *not* happen with optical imagery, because the normals to the planes used for intersection depended on the object point *j* as well as on the acquisition geometry. That was the reason the determinants of much larger matrices were needed to retrieve invariants in the previous formulation (Barrett *et al.*, 1990). Although frame optical imagery is not amenable to the simple approach developed here, it should however be noted that strip electro-optical imagery *is* amenable to a similar approach. In that case, one condition equation for image *i* can be used:

$$0 = (\mathbf{X}_j - \mathbf{S}_i - \mathbf{v}_i t_{ij}) \cdot \mathbf{v}_i. \tag{18}$$

This equation describes the instantaneous plane at time t_{ij} that passes through the sensor and is perpendicular to the sensor's velocity vector. When this equation is rewritten

$$v_i^2 t_{ij} = -\mathbf{S}_i \cdot \mathbf{v}_i + \mathbf{v}_i \cdot \mathbf{X}_j, \tag{19}$$

it is clear that three images made with linearly independent vectors $\mathbf{v}_i$ will permit a 4 by 4 matrix equation analogous to Equation 9. A ratio of determinants of the left-hand side of the equation (which consists of time measurements and a known platform speed) is then equal to a ratio of volumes in object space, as was the case in SAR. Note that, once again, the method is based on the parallelism of all the broadside planes from a single sensor (assumed to move in a straight line).

By examining matrix **F** for the SAR images, it is possible to determine conditions for geometric strength of the volume-ratio computation. The determinant of **F** is proportional to the determinant of the 3 by 3 matrix consisting of the velocity vectors $\mathbf{v}_i$ of the two platforms and the stereo-base vector $\mathbf{S}_2 - \mathbf{S}_1$ between the platforms. Hence, the greatest geometric strength is expected when these three vectors are orthogonal to each other. Conversely, no volume ratio is defined when any two of these vectors are parallel to each other, for then the determinant of **F** is zero. In particular, the methods of the preceding section do not apply to acquisition geometries in which the velocity vectors of the platforms are parallel to each other. However, the addition of more images and more object points will enhance the geometric strength even if some of the velocity vectors are parallel to each other. Such an addition will enlarge (from 4 to some number *n*) the column dimensions of matrices **G** and **F** in Equation (9), but then the equation can be rendered into a 4 by 4 matrix equation by premultiplying both sides by a constant 4 by *n* matrix. The computed 4 by 4 matrix left-hand side can then be used to compute determinants, which as before are proportional to the object-space volumes.

CONCLUSION

The purpose of this article has been to develop the invariant relationship existing in SAR imagery, and to demonstrate a simple example of its application to the problem of detecting misidentified control points in a STAR-1 image. The working of the simple example suggests that the method may be practical, particularly in view of our error analysis using SAR image-coordinate measurement errors. Ultimately, a statistical evaluation of the method should also be performed with consideration of the geometry (perspective of the template image and control point distribution), as well as measurement error in the ground-control object-space coordinates.

Other applications of the volume-ratio invariance include classification of manmade objects. In this case, one could construct a library of template images and their corresponding *V*-ratios. One could then compare the *D*-ratios in a SAR image to each object in the library. This of course requires identification and mensuration of distinctive points such as the bow, stern, or mast of a ship. It also requires a much finer SAR resolution than is available in the STAR-1 system discussed here.

The extraction of invariants from imagery in the way outlined in this paper is an analog of relative orientation in frame optical imagery. The method provides information about object space without prior resection. It also seems to be computationally robust, judging from the simulation results and error analysis presented here.

SAR imagery particularly lends itself to classification methods of this kind: the invariance relationships are simple, imaging though cloud cover is practical, and the image resolution is invariant with respect to slant range.

REFERENCES

Ausherman, D. A., A. Kozma, J. L. Walker, H. M. Jones, and E. C. Poggio, 1984. Developments in Radar Imaging, *IEEE Transactions on Aerospace and Electronic Systems AES-20*, pp. 363–400.

Barrett, E. B., P. M. Payton, N. N. Haag, and M. H. Brill, 1991. General Methods for Determining Projective Invariants in Imagery, *Computer Vision, Graphics, and Image Processing*, in press.

Brill, M. H. 1987. Triangulating from Optical and SAR images Using Direct Linear Transformations, *Photogrammetric Engineering & Remote Sensing* Vol. 55, pp. 1097–1102.

Brill, M. H., and J. R. Williamson, 1989. Multi-Sensor DLT Intersection for SAR and Optical Images, *Photogrammetric Engineering & Remote Sensing*, Vol. 55, No. 2, pp. 191–192.

Deming, W. E., 1948. *Statistical Adjustment of Data*. John Wiley & Sons, Inc., New York, pp. 39–40.

Duda, R. O., and P. E. Hart, 1973. *Pattern Classification and Scene Analysis*. John Wiley & Sons, New York.

Munson, D. C., and R. L. Visentin, 1989. A Signal Processing View of Strip-Mapping Synthetic Aperture Radar, *IEEE Trans. Acoustics, Speech, and Signal Processing*, Vol. 37, No. 12, pp. 2131–2147.

Nichols, A. D., J. W. Wilhelm, T. W. Gaffield, D. R. Inkster, and S. K. Leung, 1986. A SAR for Real-Time Ice Reconnaissance, *IEEE Trans. Geoscience and Remote Sensing*, Vol. GE-24, No. 3, pp. 383-389.

Slama, C. C (Ed.), 1980. *Manual of Photogrammetry*, Fourth Edition, American Society of Photogrammetry, Falls Church, Virginia.

(Received 5 June 1990; revised and accepted 19 October 1990)